Proposal of an engineering design approach for non-metallic fiber reinforced concrete: through experimental study and numerical modelling on UHPFRC

W.S.A. Nana[1], D. Starostina[2], S. Herbe[2], F.L. Zhou[1], J.N. Rivoal[2], E. Bonnet[1], L. Trucy[1]

[1]Holcim Innovation Center HIC, 38090 Saint Quentin Fallavier, France.
[2]Lafarge France, 38291 Saint Quentin Fallavier, France.

serge.nana@holcim.com; darja.starostina@lafarge.com; simon.herbe@lafarge.com; fulei.zhou@holcim.com; jean-nicolas.rivoal@lafarge.com; emmanuel.bonnet@holcim.com; laurence.trucy@holcim.com

Abstract

Without change there is no innovation, creativity, or incentive for improvement, while our future economic growth relies on innovation and competitiveness. Fiber-reinforced concrete (FRC) clearly appears today as a promising mechanical and economical alternative to the conventional reinforcement steel mesh. However there is still a lack of a unified design philosophy adapted to this material. Model Code 2010 is one of the most widespread designing guidelines but established on the basis of steel FRC. Based on the Model Code guidelines, the current Eurocodes are also being revised and for the first time Eurocode 2 will be extended with a harmonized annex covering FRC with metallic fibers but not taking in consideration non-metallic fibers. Non-metallic fibers are taking some of the market share from steel FRC and this is due to their non-negligible performance and ductility in a concrete matrix, their resistance to alkali attack, and their relatively low cost. It therefore becomes essential to be able to rely on design guidelines adapted to these types of fibers because this absence significantly limits their use. In this study, the Model Code recommendations are adapted to the case of non-metallic fibers to provide engineers with simplified tools. A new adapted multi-linear stress-crack opening relationship was proposed, based on experimental studies and non-linear finite element modelling. The Model Code minimum ductility requirements for FRC use in structural applications have also been adapted to the case of non-metallic fibers following Hillerborg's concept of fracture energy and a new proposal of ductility classification was made.

Keywords: non-metallic fibers; finite element; design; PVA; polyproplynene; glass; aramid.

1 Introduction

« Dare, progress is at this price ». This is especially the case for fiber-reinforced concrete (FRC), which brought today a new on how to build, and clearly appears as a promising mechanical and economical alternative to the conventional reinforcement steel mesh used in various civil engineering applications. The main benefits associated with the use of fibers can be summarized in thickness reduction so lightweight elements, no cover limitations sometimes restrictive for durability reasons in thin sections, design freedom in architectural forms, avoiding complex reinforcement detailing with a reduction of man-activity in the reinforcement arrangement. Due to a higher elasticity modulus and tensile strength, steel fibers have become the most employed type of fiber. However, non-metallic fibers are starting now to gain popularity due to their non-negligible performance and ductility in a concrete matrix, their resistance to alkali attack, and their relatively low cost. These non-metallic fibers are taking some of the market share from steel fibers, representing roughly 30% of the Ultra High-Performance Fiber-Reinforced Concrete (UHPFRC) market for example, and are mainly used for façade applications. Although there is a growing interest in non-metallic fiber reinforced concretes, its use is sometimes affected by obstacles related to the fact that there is no unified design guidelines adapted to these types of fibers. The Model Code 2010 **(Model Code 2010, 2012)** is one of the most widespread designing guidelines of FRC, but established on the basis of steel FRC, with a monotonic softening post-cracking behaviour in uniaxial tension. Based on the Model Code guidelines, the current Eurocodes are also being revised

and for the first time Eurocode 2 will be extended with a harmonized annex (annex L) covering FRC. However, it also covers only the case of steel FRC and the case of non-metallic fibers is not assessed. At the French national level, there is already a standard for UHPFRC (**NF P 18-710, 2016), (NF P 18-470, 2016**). But once again, this standard only deals with the case of metallic fibers. It therefore becomes essential to be able to rely on design guidelines adapted to the case of non-metallic fibers which behaviour, for the most part, is different from that of steel FRC. For true innovation, research work interactions, conflicts, arguments, debates are needed, and the main purpose of this study comes as a proposal of adaptation of the Model Code for the case of non-metallic fibers. Firstly, a new adapted multi-linear stress-crack opening relationship in tension was proposed, based on experimental studies and non-linear finite element (FE) modelling using an elastoplastic concrete model with damage. The different material's behaviours are reproduced using the FE method and an inverse analysis strategy. Secondly, the Model Code minimum ductility requirements for FRC use in structural applications have also been adapted to the case of non-metallic fibers following Hillerborg's concept of fracture energy and a new proposal of ductility classification was made. Indeed, due to the first drop observed in most of the FRC with non-metallic fibers, the Model Code requirements in its current state should be penalizing for these types of fibers or simply not appropriate. In the present work, the behaviours of five (05) types of non-metallic fibers in an Ultra-High Performance Concrete (UHPC) matrix are studied for the proposals made: PVA, glass, polypropylene, basalt and aramid.

2 Experimental program

2.1 Fibers properties and mixture proportion

The five types of non-metallic fibers (PVA, glass, polypropylene, basalt, aramid) were used to attain 3.0% of fiber volume fraction, corresponding respectively to dosages of 39.3 kg/m^3, 57 kg/m^3, 27.3 kg/m^3, 58.5 kg/m^3 and 41.7 kg/m^3. Note that, thanks to its optimized granular packing and low W/C ratio (0.18 to 0.28), an UHPFRC has an excellent strength, achieving compressive strength more than 150 MPa, tensile strength more than 6.0 MPa and excellent durability with respect to chloride ion penetration and freeze-thaw cycles. Today, most of the characteristic compressive strengths of UHPFRC with non-metallic fibers are between 100 MPa and 130 MPa. Although the performance is slightly below, the compressive strength is rarely critical for the design. The materials used for the study are of local origin, France. A premixed ready to use from Lafarge was retained, commercialized as «Ductal Envelope White». This premixed is composed of a white cement, a limestone filler and fine sand. **Figure 1** and **Table 1** depict the geometry and properties of all the fibers.

Table 1 : Mechanical and physical properties of the non-metallic fibers

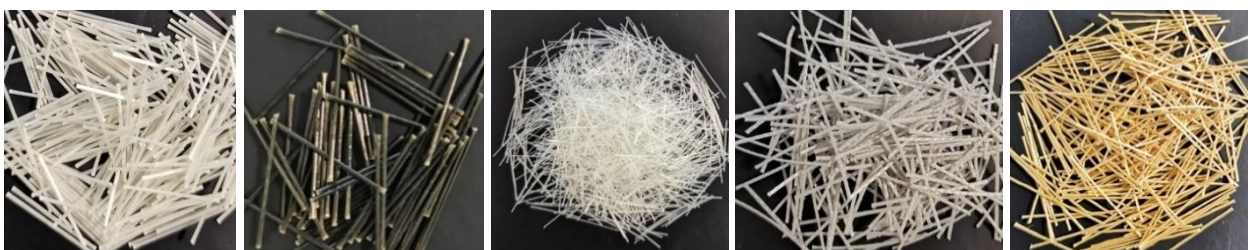| Fiber type	Density [kg/m^3]	Volume fraction[%]	Dosage [kg/m^3]	Length [mm]	Diameter [mm]	Tensile Strength[MPa]	Modulus of elasticity[GPa]	Ultimate elongation[%]
PVA	1310	3.0	39.3	12	0.17	1000	30.0	7.0
Polypropylene	910	3.0	27.3	24	0.50	640	12.0	15.0
Basalt	1950	3.0	58.5	20	0.62	1405	41.9	3.5
Glass	1900	3.0	57.0	20	0.30	1330	46.0	3.1
Aramid	1390	3.0	41.7	20	0.34	1920	53.0	4.0

Figure 1 : (a) Glass; (b) basalt; (c) PVA; (d) polypropylene; (e) aramid

2.2 Specimen preparation and test setup

The post-cracking tensile resistance is a fundamental mechanical property of UHPFRC and its proper consideration in design calculations can lead to a more efficient design. In this study, the tensile performance of the UHPFRC was evaluated by performing 3-point bending tests on prismatic samples with dimensions of 280mm×70mm×70mm and a span's length of 210 mm. A notch of 7 mm depth was cut in the middle of the samples to control the crack initiation and propagation. A total of 6 prismatic samples for each type of fibers were tested. According to (**NF P 18-470, 2016**) recommendations, the width of the square section must be between 5 and 7 times the length of the longest fibers. However, in this study, a similar section of 70mm×70mm was considered for all the fibers, also knowing that in the majority of UHPFRC applications, the thicknesses rarely exceed 7cm. It must be noted that a direct tensile test would have provide the most reliable behaviour of the UHPFRC. However, this test is very sensitive, with a dependency of results on the samples shape, hard to control the stability of the load-displacement response and ensure uniform repartition of stress through the section, which makes it difficult to conduct. Consequently, simpler methods have therefore been developed to indirectly assess the tensile properties of UHPFRC like the 3-point bending test. The load was applied at a constant displacement rate of 0.15 mm/min. However, the stresses obtained from such tests are pseudo-stresses that are not physical and are just computational stratagem. The goal of an inverse analysis performed numerically in our study is therefore to find the true tensile values of the post cracking constitutive law that allow the best fit to the experimental results.

3 Experimental results

3.1 Load-crack opening relationships

Figure 2 gathers the flexural stress – crack mouth opening displacement (σ_{fl}-w) curves obtained for all fibers. According to (**NF P 18-470, 2016**), for the 3-points bending tests, a proposed relationship also exist that relates w and midspan displacement f. Knowing the displacement f_o corresponding to the end of the elastic domain, the crack opening w is determined by the following relation: $W = (4/3) \times 0.9 \times (f - f_0)$. The flexural tensile stresses σ_{fl} are conventionally obtained by assuming a linear stress distribution over the midspan cross section, with $\sigma_{fl} = M/W$, where M is the midspan bending moment and W is the section modulus of the notched cross section. Following this assumption, the mean residual flexural tensile strengths are calculated as per the following equation, where σ_{fl} [MPa] is the residual flexural tensile stress. F [N] is the corresponding load, l [mm] is the span length (210 mm), b [mm] is the specimen width (70 mm) and h_{sp} [mm] is the distance between the notch tip and the top of the specimen (63 mm) : $\sigma_{fl} = (3 \times F_j \times l)/(2 \times b \times h_{sp}^2)$.

3.2 Material performances and evolution of residual strengths

From the results obtained (**Figure 2**), it can be noted that area under the post-peak region is larger with aramid fibers, indicating higher fracture energy and therefore greater ductility at the structural level. It should also be noted that the post-cracking behaviour is first marked by a drop after attaining the flexural tensile load σ_{fl-LOP}, which follows a strength recovery. The use of PVA and aramid fiber reinforced concrete leads to a smaller drop in load after cracking. (**Leung and Ybanez, 1997**) showed in their study that this first drop before recovering could be linked to the fact that the engagement properties of the non-metallic fibers are affected by the flexibility of these fibers having low stiffness compared to steel fibers. At first cracking, some fibers are likely oriented in non-orthogonal directions to the crack. These fibers had to become bent around the matrix entrance points at both sides of the crack and become aligned with the direction of the load before becoming effective and this character is typical of flexible fibers. Given that these fibers have some finite stiffness, this phenomenon does not happen instantly, and some crack opening is required to allow

this alignment to occur. This explains the need for a relatively large crack opening before fiber engagement in relation to steel FRC. In addition, especially for UHPC, high quantity of energy is released after cracking, which could also accentuate the level of this first drop compared to ordinary strength concrete.
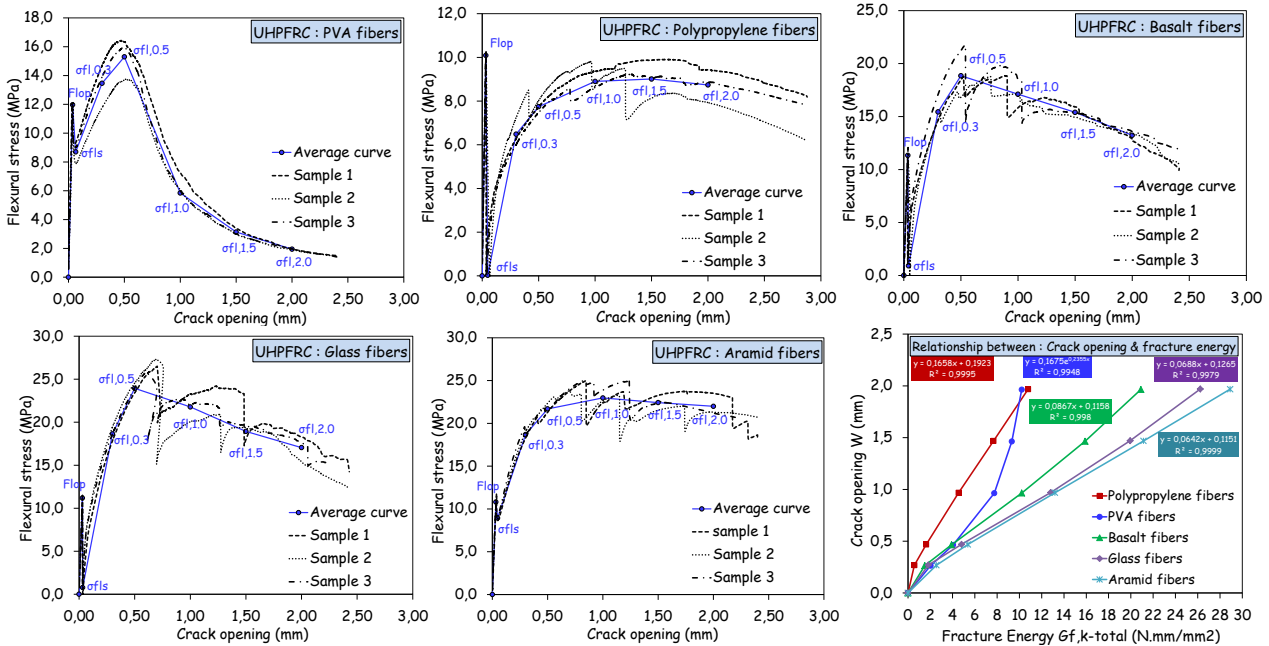

Figure 2 : (a) Three-point bending tests results; (b) Evolution of crack width with fracture energy

Table 2 : Main values of the three-point bending tests, & crack opening = f (Gfk,fl) with $G_f = G_{fk,fl}$

Fiber type	Cracking Strength Flop,m [MPa]	Post-cracking σflm,max [MPa]	Fracture energy Average Gfm,fl [N/mm]	Fracture energy Charact Gfk,fl [N/mm]	Crack opening W= f(Gfk,fl) [mm]	Ductility Class
PVA	11.9	15.3	14.6	10.2	$W=0.17e^{0.24Gf}$ for w>0.27mm	Level n°1
Polypro	10.1	9.0	15.4	10.8	W=0.17Gf+0.19 for w>0.27mm	Level n°1
Basalt	11.3	18.9	29.9	20.9	W=0.09Gf+0.12 for w>0.27mm	Level n°3
Glass	11.2	23.9	37.5	26.2	W=0.07Gf+0.13 for w>0.27mm	Level n°4
Aramid	10.8	22.4	41.3	28.9	W=0.06Gf+0.12 for w>0.27mm	Level n°4

3.3 Proposition of ductility requirement for non-metallic fibers and classification

In the (**Model Code 2010, 2012**), there is a minimum ductility requirement for FRC to be used in structural applications to substitute conventional reinforcement. Two conditions must be met: $f_{R1,k}/f_{LOP,k} > 0.4$ and $f_{R3,k}/f_{R1,k} > 0.5$. With $f_{LOP,k}$ the flexural cracking load, $f_{R1,k}$ the residual tensile flexural stress for crack opening of 0.5mm, and $f_{R3,k}$ the residual tensile flexural stress for crack opening of 2.5mm. (**Nana et al, 2021**) have shown in their study that these requirements may not be suitable for non-metallic fiber cases. Indeed, these requirements have been established based on steel FRC with monotonic post-cracking behaviour and is therefore not suitable for the case of non-metallic FRC with non-monotonic behaviour marked by a first pronounced drop before strength recovering. The first condition ($f_{R1,k}/f_{LOP,k} > 0.4$) might not be fulfilled while the second largely. This was easily noticed in their study by adopting Hillerborg's concept of fracture energy G_f (**Hillerborg et al, 1976**) in fracture mechanics. The fracture energy (G_f) is computed as the area under the flexural post-cracking curve, and represents the total energy dissipated by concrete after cracking up to failure assumed to occur at a crack opening of 2.5 mm. The greater the fracture energy, the greater the ductility of the structure. Parameter G_f appears consequently as a better indicator of non-metallic FRC ductility. For example, a couple of values for steel FRC ($f_{LOP,k} = 4.3\,\text{MPa} - f_{R1,k} = 1.72\,\text{MPa} - f_{R3,k} = 0.86\,\text{MPa}$) meets the requirements of the Model Code

2010 and the corresponding fracture energy $G_f = 4.10$ N.mm/mm². In contrast, the data for non-metallic FRC ($f_{LOP,k} = 4.14$ MPa $- f_{R1,k} = 1.37$ MPa $- f_{R3,k} = 1.97$ MPa) lead to an inability to be used in structural applications. However the fracture energy obtained $G_f = 4.70$ N.mm/mm² is higher than that of the first case and shows here a certain inconsistency (**Nana et al, 2021**). In addition, the Model Code allows crack openings up to 2.5 mm in its ductility criterion, which might not always be achieved with some non-metallic fibers, such as PVA for example in our study. It therefore appears the need to redefine the Model Code 2010 requirements for the case of the non-metallic FRC. A minimum value of fracture energy $G_{fk-fl-min}$ to be observed for any structural application can be defined based on the minimum requirements of the Model Code 2010. Considering an UHPFRC with minimum characteristic compressive strength $f_{ck} = 100$ MPa, the value of f_{LOP} is generally obtained by a 4-point bending test according to (**NF P 18-470, 2016**) and in general a minimum common value obtained is $f_{LOP,k-min} = 12.0$ MPa. The minimum couple that will meet the Model Code ductility requirements would be : $f_{LOP,k} = 12.0$ MPa $- f_{R1,k} = 4.80$ MPa $- f_{R3,k} = 2.40$ MPa and by considering a crack opening up to 2.0mm, the fracture energy will be : $G_f = 9.60$ N.mm/mm². A new type of classification is proposed here and depends directly on the fracture energy value $G_{f,k}$, and not on the two Model Code conditions in the form of ratios. A minimum value of $G_{fk-fl-min}$ must be respected for non-metallic UHPFRC to be used in structural applications and is indicated below.

$$G_{fk-fl} = \int_{w=0 \text{ mm}}^{w=2.0 \text{ mm}} \sigma(w)dw$$

$$G_{fk-fl-min} = \int_{w=0 \text{ mm}}^{w=2.0 \text{ mm}} \sigma(w)dw \geq \max\ (10.0 \,;\, 0.02 f_{ck} + 8.0)\ \text{N.mm/mm}^2$$

The proposition of ductility classification for UHPFRC with non-metallic fibers is given below. Compared to (**Model Code 2010, 2012**), it has the advantage of being more suitable for non-metallic FRCs having a non-monotonic behavior with drop. And compared to (**NF P 18-710, 2016**), (**NF P 18-470, 2016**), it has the advantage of differentiating in term of ductility strength, different non-metallic UHPFRCs already fulfilling the criterion on $G_{fk-fl-min}$. The designer has to specify the value of G_{fk-fl} and the associated ductility class. The value of G_{fk-fl} is computed from the flexural stress – crack mouth opening displacement (σ_{fl}-w) curves. The characteristic curves must be used and is defined by some reference points : $f_{LOP,k}$ the flexural cracking load, and the residual tensile flexural stresses $\sigma_{fl,0.3}$, $\sigma_{fl,0.5}$, $\sigma_{fl,1.0}$, $\sigma_{fl,1.5}$, $\sigma_{fl,2.0}$, defined as the stresses values at crack openings 0.3mm, 0.5mm, 1.0mm, 1.5mm and 2.0 mm respectively. The drop point after first cracking must also be considered.

Ductility – Level n°1: $10.0 \leq G_{fk-fl} < 13.5$ N.mm/mm²
Ductility – Level n°2: $13.5 \leq G_{fk-fl} < 18.5$ N.mm/mm²
Ductility – Level n°3: $18.5 \leq G_{fk-fl} < 25.0$ N.mm/mm²
Ductility – Level n°4: $25.0 \leq G_{fk-fl} < 34.0$ N.mm/mm²
Ductility – Level n°5: 34.0 N.mm/mm² $\leq G_{fk-fl}$

4 Numerical modeling

Nonlinear finite element modelling and an inverse analysis procedure were used to model the post cracking behaviour of UHPFRC. The goal here is to use the numerical model based on the material tests carried out, to propose a reliable analytical stress-crack opening law (σ-w) for elements design in UHPFRC with non-metallic fibers. The numerical investigations were conducted using the concrete damaged plasticity (CDP) model available in the finite element (FE) software Abaqus.

4.1 Theoretical background of the CDP model

The CDP model is part of the continuous approaches for crack modeling in concrete. The concrete is considered as a continuous space and its nonlinear behaviour is inserted in the material law behaviour. We thus avoid the discontinuous character caused by the crack, by homogenizing the constitutive law on a finite field. The model is based on an elasto plasticity-based damage model (**Lubliner et al, 1989**) and seems to be the most suitable for quasi-brittle materials, compared to the "smeared cracking model" also available in Abaqus **(Nana et al, 2021), (Wosatko et al, 2019)**. A constitutive law can be established to correlate Cauchy tensor of stress to the tensors of strains according to:

$$\sigma_t = (1 - d_t)E_0 : \left(\varepsilon_t - \varepsilon_t^{pl}\right) ; \sigma_c = (1 - d_c)E_0 : \left(\varepsilon_c - \varepsilon_c^{pl}\right)$$

$$F_{CDP} = \frac{\bar{q} - 3\alpha\bar{p} + \beta(\tilde{\varepsilon}^{pl})\langle\hat{\bar{\sigma}}_{max}\rangle - \gamma\langle-\hat{\bar{\sigma}}_{max}\rangle}{1 - \alpha} - \bar{\sigma}_c\left(\tilde{\varepsilon}_c^{pl}\right) = 0; G_{CDP} = \sqrt{(e\sigma_{t0}\tan\psi)^2 + \bar{q}^2} - \bar{p}\tan\psi$$

A Drucker-Prager criterion-based yield function F is implemented in the CDP model. Given the cohesive-frictional character of concrete, a non-associated flow rule with the help of a plastic potential function G is used. In the present study, the following values: $\sigma_{b0}/\sigma_{c0} = 1.16, K_c = 0.667$, $\psi = 37°$ and $e = 0.1$ have been retained. More details on the CDP model and the calibration procedure can be found in **(Nana et al, 2021)**.

4.2 Proposition of tensile stress-crack opening laws using inverse analysis

The inverse analysis is performed in our study using the nonlinear finite element modeling to find the direct tensile test values that allow best fit to the experimental flexural results. For this purpose, a multilinear diagram for the direct tensile law is proposed. A minimum error in the simulations is verified to be less than 5%. The mean value of compressive strength for all the samples was quasi $f_{cm} = 115$ MPa and the Young modulus $E_0 = 50$ GPa. The concrete region of the samples was meshed using 8 node reduced integration brick elements and the mesh size was 10 mm (**Figure 3**), chosen through a mesh convergence study. The simulations were conducted with an explicit quasi-static solution technique. The noticeable advantage of the explicit analysis compared to a conventional implicit method is the absence of convergence problems, and reliable results for shorter computation times. This is achieved in our study by applying the load as a low velocity in a displacement-controlled analysis. The kinetic energy is verified to be negligible (<5%) compared to the internal energy. As shown in **Figure 4**, a very good prediction was obtained for the inverse analysis. These results reveal that the proposed trilinear diagram shown in **Table 3** is able to predict, with enough accuracy, the post cracking behaviour of the tested UHPFRC specimens.
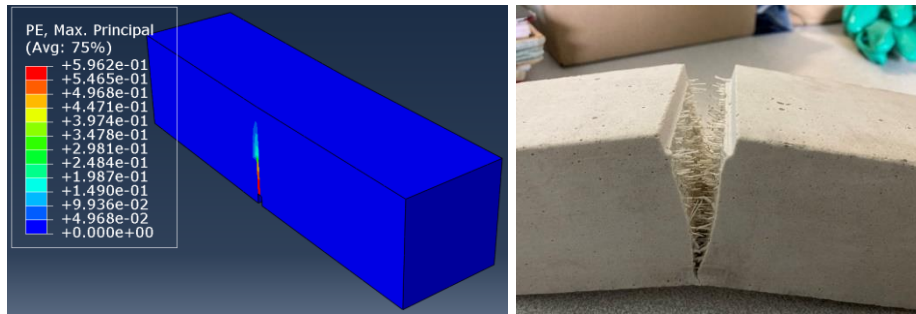

Figure 3 : Finite element model of the prismatic beams

*Note that in **Table 3** below, for UHPFRC with drop after the first cracking more than 60%, then $\sigma_{tm,s} = 0.01 \times \sigma_{tm,0.3}$, if not the following value must be considered, $\sigma_{tm,s} = 0.45 \times \sigma_{tm,0.3}$.

Table 3 : Proposed new approach for defining the post cracking σ-w diagram, mean values

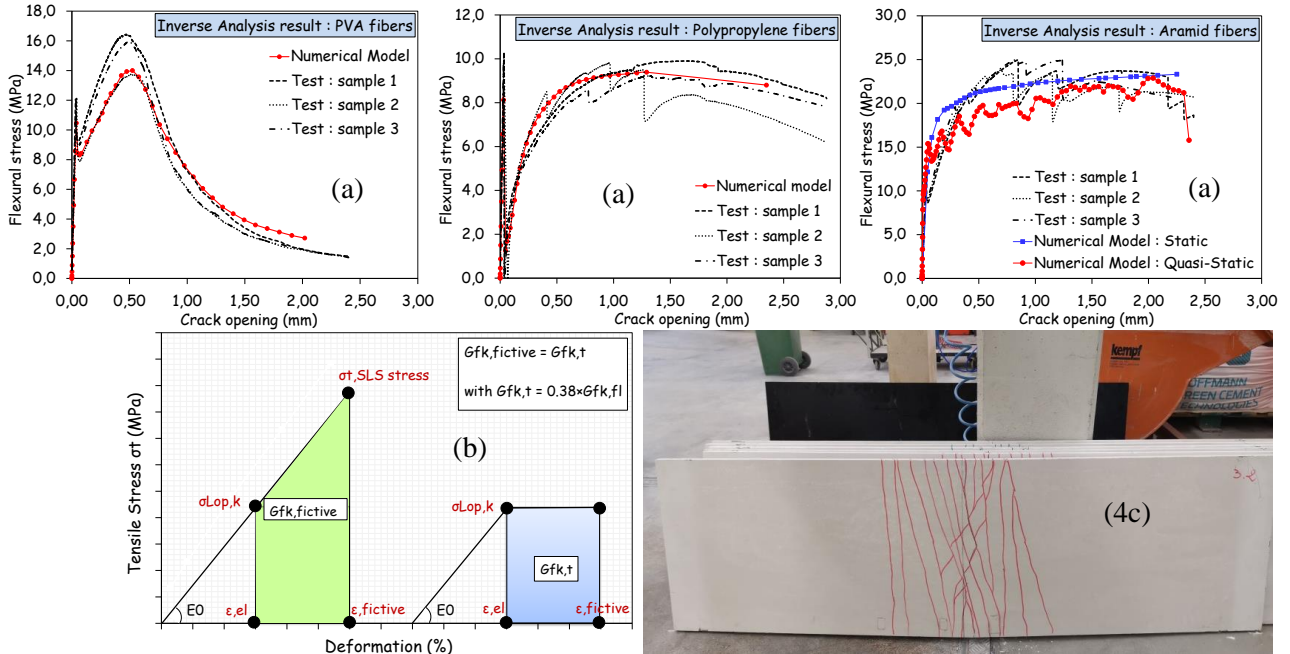| $\sigma_{LOP,m}$ [MPa]	$W_{el} = 0.0$ [mm]
*$\sigma_{tm,s} = 0.45 \times \sigma_{tm,0.3}$ [MPa]	$W_s = W_{0.3}/10$ [mm]
$\sigma_{tm,0.3} = 0.38 \times \sigma_{flm,0.3}$ [MPa]	$W_{0.3} = 0.3$ [mm]
$\sigma_{tm,0.5} = 0.38 \times \sigma_{flm,0.5}$ [MPa]	$W_{0.5} = 0.5$ [mm]
$\sigma_{tm,1.0} = 0.38 \times \sigma_{flm,1.0}$ [MPa]	$W_{1.0} = 1.0$ [mm]
$\sigma_{tm,2.0} = 0.38 \times \sigma_{flm,2.0}$ [MPa]	$W_{2.0} = 2.0$ [mm]

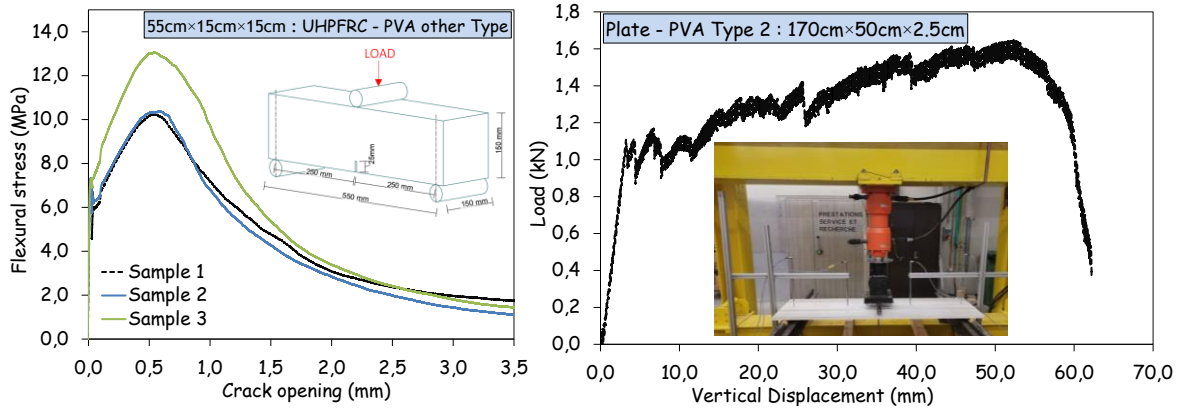**Figure 4 :** (a) Results of the numerical modelling; (b) Proposed method to calculate crack opening W_{max}

Figure 5 : Plate 170cm×50cm×25mm with PVA-other type 2: Load-displacement; (4c) cracking pattern

5 Proposition of design methodology

Step n°1: Determination of ductility class

The designer has to specify the value of fracture energy G_{fk-fl} and the associated ductility class according to the classification method proposed in the present study. Note that for all design, characteristic values must be used and not mean values.

Step n°2: Design at Serviceability Limit State (SLS)

Under SLS combinations, there is no cracking if the acting tensile stress $\sigma_{t,SLS}$ is less than the characteristic cracking strength $\sigma_{LOP,k}$ with. The partial safety factor to be considered is $\gamma_F = 1.0$. If $\sigma_{t,SLS}$ exceeds $\sigma_{LOP,k}/\gamma_F$, then there is cracking and the maximum crack opening W_{max} must not

7

exceed 0.3mm. A method for calculating the crack opening is proposed below by integrating a fictitious elastic energy Gfk,fictive which must equilibrate the fracture energy associated with cracking Gfk,t (**Figure 4b**). It should be noted that the fictitious deformation is by hypothesis an increase in the elastic deformation to take into account the amplifying effects of a cracked inertia. It should be noted that Gfk,t is the equivalent fracture energy under a tensile curve from that obtained under flexural curve Gfk,fl. Knowing the relationship between crack opening and fracture energy (**Table 2**), one can then calculate the crack opening generated by the excess elastic stress.

$$W_{fictive} = (\varepsilon_{fictive} - \varepsilon_{el}) \times l_c; \text{With } \varepsilon_{el} = \sigma_{LOP,k}/E_0 \text{ ; } \varepsilon_{fictive} = 19 \times \sigma_{t,SLS}/E_0 \text{ ; } l_c = 0.67h$$

$$G_{fk,fictive} = W_{fictive} \times \frac{(\sigma_{t,SLS} - \sigma_{LOP,k})}{2} + W_{fictive} \times \sigma_{LOP,k} = G_{fk,t} \text{ ; With } G_{fk,fl} = G_{fk,t}/0.38$$

$$W_{max-aramid} = 0.06 \times G_{fk,fl} + 0.12 \text{ ; } W_{max-polypro} = 0.17 \times G_{fk,fl} + 0.19$$

Step n°3: Design at Ultimate Limit State (ULS)

Under ULS combinations, cracking of the concrete is allowed. The ULS design acting moment M_{ED} must be compared to the moment capacity of the UHPFRC, M_{RD}. A sectional analysis must be performed to determine the moment capacity/tensile strain curves. The compressive behaviour recommended in (**NF P 18-710, 2016**) can be used. The tensile behaviour is the one corresponding to the proposed new approach. The UHPFRC tensile stress-crack opening laws (σ-w) are converted to stress–strain (σ-ε) laws through the characteristic length taken as $l_{cs} = 0.67 \times h$ according to $\varepsilon = w/l_{cs}$ where h is the structure thickness. The partial safety factor to be considered is $\gamma_F = 1.5$. In addition to the partial safety factor, to take into account the influence of fiber orientation, the non-isotropy, a K safety factor for global effects must be used. Factor K should be determined from the tests conducted on the placement methods.
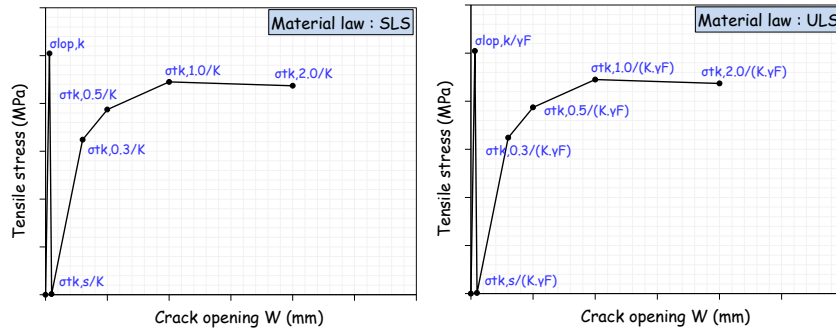

Figure 6 : Material constitutive tensile law for design at SLS & ULS

References

- Model Code 2010. Final Draft, fib bulletins 65 and 66. Int Fed Struct Concr Fib 2012.
- NF P 18-710, Complément national à l'Eurocode 2 - Calcul des structures en béton: règles spécifiques pour les Bétons Fibrés à Ultra-Hautes Performances (BFUP), 2016.
- NF P 18-470, Béton - Béton fibrés à Ultra-Hautes Performances - Spécification, performance, production et conformité, Juillet 2016.
- Nana, W. S. A., Tran, H. V., Goubin, T., Kubisztal, G., Bennani, A., Bui, T. T. & Limam, A. (2021, August). Behaviour of macro-synthetic fibers reinforced concrete: Experimental, numerical and design code investigations. In Structures (Vol. 32, pp. 1271-1286). Elsevier.
- Wosatko, A., Winnicki, A., Polak, M. A., & Pamin, J. (2019). Role of dilatancy angle in plasticity-based models of concrete. Archives of Civil and Mechanical Engineering, 19, 1268-1283.
- Lubliner J, Oliver J, Oller S, Onate E. A plastic-damage model for concrete. Int J Solids Struct 1989; 25 (3):299–326.
- Leung CK, Ybanez N. Pullout of inclined flexible fiber in cementitious composite. J Eng Mech. 1997. 123. 239–46.
- Hillerborg A, Modeer M, Petersson P-E. Analysis of crack formation and crack growth in concrete by means of fracture mechanics and finite elements. Cem Concr Res 1976;6(6):773–81.